IEEE Access
Multidisciplinary ⋮ Rapid Review ⋮ Open Access Journal

Received November 24, 2020, accepted December 4, 2020, date of publication December 10, 2020,
date of current version December 29, 2020.

Digital Object Identifier 10.1109/ACCESS.2020.3043824

Switchable Slant Polarization Filtering Antenna Using Two Inverted Resonator Structures for 5G Application

DWI ASTUTI CAHYASIWI, (Student Member, IEEE), FITRI YULI ZULKIFLI, (Senior Member, IEEE), AND EKO TJIPTO RAHARDJO, (Member, IEEE)
Department of Electrical Engineering, Universitas Indonesia, Depok 16424, Indonesia

Corresponding author: Eko Tjipto Rahardjo (eko@eng.ui.ac.id)

This work was supported by the Publikasi Terindeks Internasional Research Grant-UI (PUTI) 2020 under Contract NKB-650/UN2.RST/HKP.05.00/2020.

ABSTRACT This study presents a novel design of two filtering antennas with a +45° and −45° slant polarization, using the co-design of a third-order filter and a rectangular patch antenna. Slant polarization is obtained by directing the surface current that flows to the radiator by applying two parallel inverted resonators in the transmission line. The resonators consist of two parallel strips with alternate open and short circuits at each end and the 45° and −45° polarization is determined from these short circuit positions. The rectangular patch antenna is fed using proximity coupling, and it is parallel to the resonators. The filtering antennas provide not only 45° slant polarization, a flat gain response but also a controllable bandwidth. Operating at 4.65 GHz for 5G application, the antennas have a controllable bandwidth range from 5.9% to 8.4% without affecting the polarization and center frequency. The gain responses are filter like and attain the maximum value of 6.82 and 6.69 dBi at 4.7 GHz. This design needs no extra component or rotation of the radiator and transmission line because the inverted resonators can switch the polarization to be +45° and −45°. The results of the 45° and −45° polarization filtering antenna simulation and experiments are consistent with each other.

INDEX TERMS Filtering antenna, 5G, inverted resonator, slant polarization, switchable polarization.

I. INTRODUCTION

Devices with multifunction features are an essential requirement for telecommunication equipment nowadays. Over the years, the co-design of a filter and antenna that produces compact and multifunctioning circuits has been explored. An antenna with 45° polarization can overcome the effect of multipath reflections in outdoor and indoor propagations. This polarization is beneficial because multipath reflection results in the alteration of the polarization from horizontal/vertical to slant polarization, which consequently degrades the performance of the received signals due to mismatch polarization. An antenna with a ±45° slant polarization has many advantages because of its better gain diversity [1], higher channel capacity [2], [3], and lower bit error rate compared with horizontal/vertical polarization [4].

Many studies have discussed methods to perform linear polarization [5]–[7] however like other filtering antennas without an extra circuit they did not provide a controllable bandwidth which is necessary in some wireless systems. A multilayer filtering antenna using a cross-radiator and square ring slot as resonators performed dual-polarization [8]; however, it did not explain about the controllable bandwidth method and the vertical/horizontal polarization could not combat the multipath fading effect. Though some studies have discussed methods to obtain ±45° polarization in a filtering antenna, these methods required a physical rotation of the radiator and feedline because the designs did not exhibit a function to control the polarization and bandwidth [9]–[12]. In [9] and [10] a filtering antenna with a 45° slant polarization was developed by rotating the

The associate editor coordinating the review of this manuscript and approving it for publication was Giorgio Montisci.

dipole antenna element, though utilizing the filtering element, no controllable bandwidth and polarization was achieved by the resonator. In [11], a rectangular patch radiator and split ring resonators rotated at ±45° were used, but these asymmetric resonator structures resulted in an unidentical *S*-parameter, gain, and radiation pattern for both polarizations, and the resonator also did not operate to control the polarization. In a dual-polarized conventional antennas, some methods did not use a filtering structure [13]–[16]. For example an omnidirectional biconical antenna in [14] additionally used a multiscreen polarizer to achieve 45° slant polarization; however, this method is complex and bulky because of its three-dimensional structure, and no filtering response was obtained. Moreover, [17] used a metallic/multiscreen dielectric parallel-piped antenna with a feeding probe and rotated the dielectric material to achieve 45° slant polarization. However, the use of eight parallel pipes not only resulted in difficulty in alignment but also a three-dimensional structure that did not support a compactness requirement. Further, [18], [19] proposed an omnidirectional antenna with four crossed-dipole elements that had more than 17% bandwidth; however, in addition to the complexity of the three-dimensional structure, which is not easy to manufacture, it also has a low gain problem (less than 1 and −1 dBi), and no filtering response or controllable bandwidth were exhibited. Other dual-polarized slant polarization antenna used cross dipole [20] but it did not perform a filtering gain response or a controllable bandwidth. Though reconfigurable slant and circular polarizations were performed with a unidirectional radiation pattern [21], the design only provided a gain less than 3 dBi and bandwidth less than 4%. An antenna with a slant polarization has been designed using characteristic modes[22], however, it has no response of gain selectivity or controllable bandwidth.

In a filtering antenna, there is no report on parallel inverted resonators that performed 45° slant polarization. Though in a previous study [23], a single strip resonator with a via hole in one of its arms, was arranged parallel to a rectangular patch radiator and performed a ±75° slant polarization, however, no orthogonal polarization was achieved. To the best of the author's knowledge, this is the first proposal of a filtering antenna that applies two strip line resonators to control the polarization; thus, there is no need for polarizer addition or physical rotation of the radiator or transmission line. Slant polarization is achieved by altering the direction of the surface current that flows to the radiator, thus altering the electrical field from vertical to ±45° polarization. The ±45° slant polarization is obtained utilizing the co-design of a third-order filter using two parallel strip resonators with an alternately open and short circuit at each arm that are also parallel to the rectangular radiator. The short circuit is represented by a via hole that is positioned inverted on each resonator's end. The position of the via hole determines the direction of the slant polarization.

The main contributions of this design are as follows:

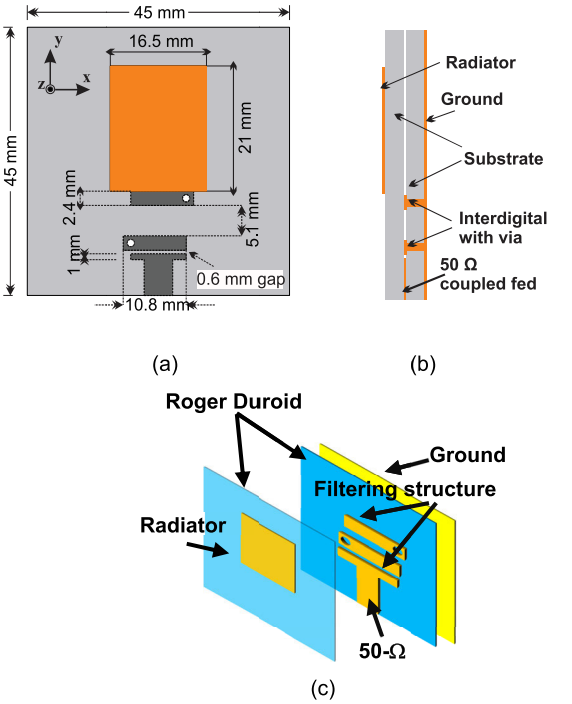

FIGURE 1. Proposed filtering antenna (a) geometry, (b) side view, and (c) perspective view.

1. The antennas apply two inverted and parallel strip resonators that perform 45° and −45° polarization; thus, there is no extra component or rotation of the radiator and feedline.
2. The design has an independently controllable bandwidth without affecting the polarization and center frequency.
3. The sharpness of the gain response at the upper and lower frequency can be controlled independently without affecting the center frequency.
4. The co-design of a strip-line with a via hole resonator and rectangular patch provides a flat gain response along the bandwidth, such as a filter response.
5. The polarization switching does not affect other antenna parameters; thus, all parameters such as reflection coefficient, gain, and radiation pattern are identical for both polarizations.

II. ANTENNA CONFIGURATION

The proposed stacked inverted filtering antenna (SIFA) depicted in Fig. 1 consists of two dielectric substrates (Roger Duroid 5880) layers with a relative permittivity of 2.2, dielectric thickness of 1.575 mm, and a loss tangent of 0.0009. As shown in Fig. 1 (a), the first layer is a 16.5 mm × 21 mm rectangular patch antenna, proximity fed by two parallel strip resonators that are coupled fed by a 50-ohm transmission line (4.9 mm). The two parallel strip resonators have a via hole at each end, which are arranged alternately. The resonator's thickness is 2.4 mm, and its length is approximately a quarter wavelength of the center frequency. The via diameter is 1.2 mm, and two layers are printed on the 45-mm × 45-mm substrate. There is a gap of 0.6 mm between the coupled feed and the first resonator. From the filter extraction,

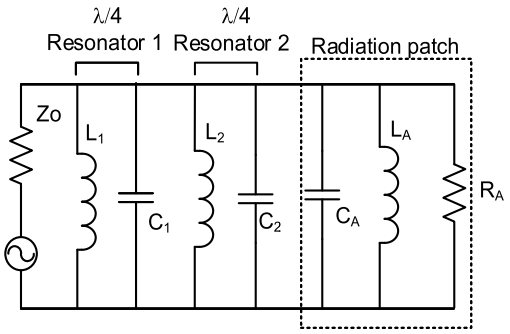

FIGURE 2. Equivalent circuit.

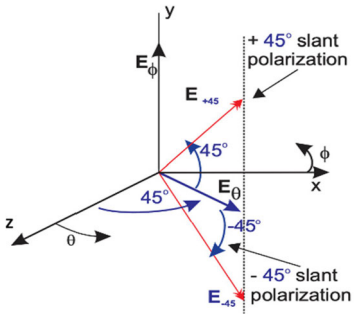

FIGURE 3. Electrical field vectors of ±45° (red vector) slant polarization definition in the far-field.

the gap between the two resonators is 5.1 mm, and there is no gap between the rectangular patch on the first layer and the second resonator. The geometry of the SIFA is shown in Fig. 1(a), while the side and perspective views are displayed in Fig. 1 (b) and (c). SIFA is based on a synthesized third-order bandpass filter; in this study, the rectangular patch radiator replaces the third resonator.

The equivalent circuit of the SIFA is shown in Fig. 2, where the radiating patch is characterized as L_A, C_A, and R_A, which are capacitively coupled fed with the second strip-line resonator (L_2 and C_2). The two adjacent λ/4 resonators are also capacitively coupled with the via hole alternately positioned at the arm of each resonator. At the first stage, the strip-line resonator, consisting of L_1 and C_1, is coupled fed by the adjacent Z_o (50 Ω) feed line.

III. SLANT POLARIZATION METHOD

The ±45° polarization scheme in the far-field is described in Fig. 3. Slant polarization of ±45° is achieved if the phase difference, δ_L, between the electric field vector in the θ (E_θ) and Φ (E_Φ) direction is 0° for 45° or 180° for −45°, as described in the following equation [24]:

$$\bar{E} = E_\theta cos(\omega t)\hat{\theta} + E_\theta cos(\omega t + \delta_L)\hat{\Phi} \tag{1}$$

where ω is the angular frequency. Slant polarization also requires $|E_\theta|$ and $|E_\Phi|$ to be equal; this can be expressed as follows [24]:

$$|E_\theta| = |E_\Phi| \tag{2}$$

Equation (2) can also be written as $|E_\theta|/|E_\Phi| = 1$.

It is comprehended that a strip line resonator with a via hole at one arm characterizes a short circuit and an open circuit at the other arms [25], and in a transmission line, an open circuit and short circuit have a 180° phase difference. Accordingly, this structure has prospective for achieving ±45° slant polarization. A stacked filtering antenna was previously designed using a single resonator based on a second-order filter [23]. Although filtering response was achieved, the design failed to perform 45° slant polarization. In the proposed design, two resonators are used based on a third-order filter, even though the optimization result shows a second order filtering antenna response, the 45° and −45° slant polarization is successfully achieved.

SIFA is designed to operate with a center frequency of 4.65 GHz, fractional bandwidth (FBW) of 6.45%, and ripple level of 0.2 dB. From [26], the parameters of the low-pass filter are $g_0 = g_4 = 1$, $g_1 = g_3 = 1.2275$, and $g_2 = 1.1525$. The external quality factor, Q_{en}, and the coupling between the two adjacent resonators, $M_{i,i+1}$, the value for which are 19.026 and 0.054, respectively, can be calculated using (3) and (4) [27]

$$Q_{en} = \frac{g_n g_{n+1}}{FBW} \tag{3}$$

$$M_{i,i+1} = \frac{FBW}{\sqrt{g_i g_{i+1}}} \tag{4}$$

The value of Q_{en}, and $M_{i,i+1}$ can be used for the filter extraction using electromagnetic simulation. By adjusting the gap between the coupled feed and the first resonator, the Q_{en} value can be obtained using the following calculation,

$$\Delta Q_{en} = \frac{f_c}{f} \tag{5}$$

where f_c is the center frequency and Δf is the 3 dB bandwidth. Meanwhile, the coupling between two adjacent resonators is obtained by varying the distance between the two resonators whose responses are then used in the following equation

$$M_{n,n+1} = \frac{f_{n+1}^2 - f_n^2}{f_{n+1}^2 + f_n^2} \tag{6}$$

where f_n and f_{n+1} are the first and second resonant frequencies, respectively. Since the rectangular patch antenna replaces the third resonator in the filter network, Q_{en} must have the same value as the quality radiation, Q_{rad}, and the coupling between the first and second resonators, $M_{1,2}$, must be equal to the coupling between the second resonator and the radiator, $M_{2,3}$. However, integration of radiator and filter is not the only design consideration for the SIFA because its purpose is also to perform a slant polarization using the resonators.

The principal technique to perform a slant polarization in the SIFA is to feed the rectangular radiator with a horizontal surface current from the resonators. This current creates a force attraction with the vertical surface current along the patch length. If the right proportion of the width and length of the radiator is combined with the gap between the antenna

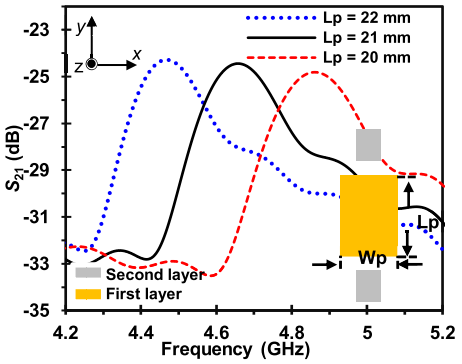

FIGURE 4. Frequency response of the rectangular patch with different L_p and constant $W_p = 3$ mm.

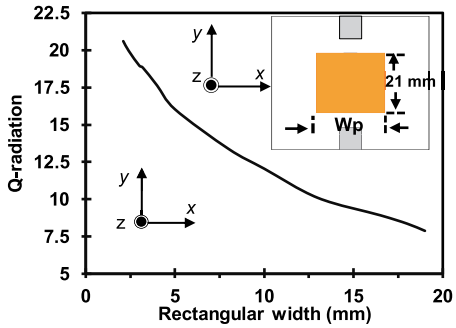

FIGURE 5. Q-radiation over the width of the rectangular radiator with a constant $L_p = 21$ mm.

and the resonators, a slant surface current is obtained. The gap between the resonator and radiator needs to be small to intensify the effect of the horizontal surface current but still has to maintain the matched condition. Those constraints drive the integration of the antenna and filter to satisfy the requirement for the slant polarization condition.

IV. DESIGN AND ANALYSIS

In this design, the horizontal surface current is represented using a strip resonator with a short circuit at the end of the resonator's arm. This is to ensure that the surface current flows to the path with less resistance. The step-by-step integration design of the two circuits is presented in the next section.

A. RADIATOR DESIGN

The antenna's patch is designed using approximation calculation of the rectangular radiator that is commonly used, where the height of the antenna determines the resonance frequency. Then the patch is extracted with proximity coupling to obtain the dimensions of the rectangular patch as shown in Fig. 4. The 4.65-GHz resonance was obtained with a patch length of approximately 21 mm. The width of the antenna determines the quality factor of the radiator. As shown in Fig. 5 and from the extraction using (5), reducing the width of antenna increases Q_{rad}. Thus, an antenna width of 3 mm is necessary to obtain Q_{rad} of 19.026 as required from the synthesis. However, this width decreases horizontal surface current force in x direction, which results in the

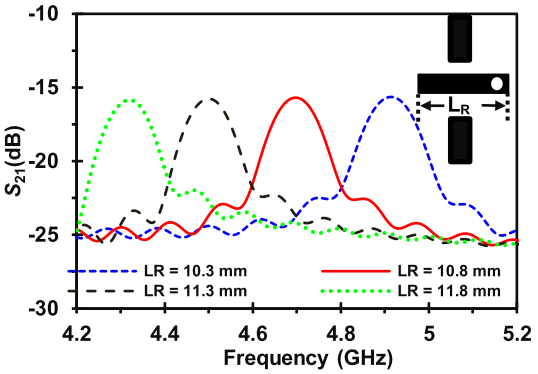

FIGURE 6. Frequency response of resonator under the different length (L_R) with a thickness of 2.4 mm.

vertical surface current in the y direction along the length of radiator being dominant. Thus, this antenna width results in vertical polarization instead of slant polarization. To obtain slant surface current on the radiator, the patch width (W_p) is driven to be far greater than 3 mm when directly tuned into the filtering circuit. Hence, only the patch length is used for the integration process. As shown in Fig. 5, increasing the radiator width decreases Q_{rad}. Consequently, the radiator actually has potential to achieve a fractional bandwidth wider than 6.45%, especially when the radiator width is adjusted to approach the radiator length and strengthen the feeding effect of the horizontal surface current.

The range of W_p is chosen under the consideration, to ensure that the surface current of the horizontal resonator has a strong effect in the x direction, W_p needs to be close to L_p. However, the W_p and L_p should not be identical because a single port feeding means that a strong current is induced mainly in the x direction and deteriorates along the length of the radiator or y direction. Thus, in this design, W_p is restricted to 15–18 mm to ensure a moderate horizontal surface current. Finally, the integration needs to achieve the filtering effect and polarization control in the radiator part.

B. FILTERING CIRCUIT DESIGN AND INTEGRATION

The first step of the filtering circuit design is to extract the external quality factor of the resonator (Q_{en}) using (5). The thickness of the resonator is set to 2.4 mm with via hole diameter of 1.2 mm, and the strip resonator length is set to approximate a quarter wavelength. The resonance of the resonator is extracted using two substrates and two ports. The response of the resonance frequency and length of the resonator is represented using S_{21}, as shown in Fig. 6, where the 10.8 mm resonator resonates at 4.65 GHz. The via hole position determines the resonance frequency because a longer distance for the current to flow to the via hole (P_k) lowers the resonance frequency. Fig. 7 shows the relation between the distance from the via hole to the edge of the strip line and the frequency response with a constant resonator length of 10.8 mm. After the length of the resonator is obtained, the coupling between the two resonators is also extracted using two substrates as shown in Fig. 8 (a) to obtain the gap

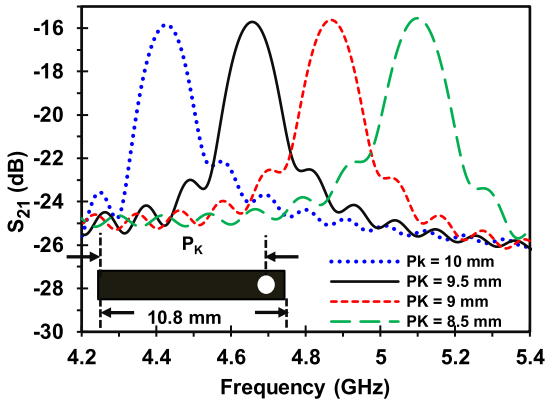

FIGURE 7. Frequency response of the resonator under different via position (P_k) with resonators length (L_R) of 10.8 mm.

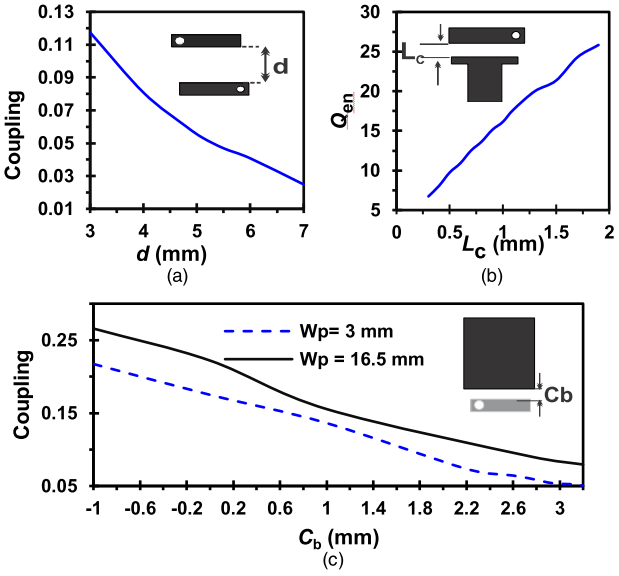

FIGURE 8. Extraction of gap between (a) two resonators (d), (b) the feedline and the first resonator (L_c) and (c) radiator and the second resonator (C_b) under different W_p.

between them. The two-peak frequency response is calculated by using (6) to obtain a value of 0.054, which results in a gap of 5.1 mm. The next step is to extract the gap between the coupled feed and resonator. The extraction is expressed by the relation between the gap and Q_{en} as shown in Fig. 8(b). Increasing the gap between the coupled feed and resonator (L_c) increases Q_{en}. The extraction obtains a 1.3 mm gap between the resonator and coupled feed to obtain $Q_{en} = 19.026$. However, to retain the horizontal surface current force, the gap is driven to be no wider than 0.8 mm and no narrower than 0.5 mm. For the conventional integration of filtering antennas, the coupling between the second resonator and the radiator should be equal to the coupling between the two resonators. However, as explain in Section IV Part A the sizes of the radiator based on extraction is unsuitable for the purpose of this design because the W_p in SIFA is driven to be wider than that in the conventional extraction, then the extraction result is left out and the gap between

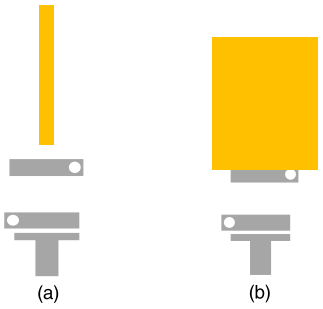

FIGURE 9. Scheme of the filtering antenna based on the (a) conventional extraction and (b) proposed method.

the radiator and the second resonator must be optimized to obtain a horizontal surface current that is required for slant polarization. Still, the different results of the two designs are presented in this study for comparison. The optimization is performed so that the gap between the coupled feed and first resonator is not too wide to strengthen the horizontal feed line.

The same condition is considered for the gap between the radiator and second resonator as shown in Fig. 8(c). Avoiding a wide gap between the resonator and antenna maintains the strength of the horizontal surface current force. This condition sacrifices the third-order filtering response of the antenna. The extraction of the coupling between the second resonator and radiator for conventional antennas is also left out in this design because the gap is arranged smaller and the width is wider to obtain matching condition and slant polarization, which could differ from the extraction results. The tuning of the S-parameter for the SIFA relies on the combination of the radiator size, gap between two resonators and gap between radiator and resonator. Arranging a gap of −0.5 to 0.5 mm between the second resonator and rectangular patch strengthens the surface current. This is also why proximity coupling is chosen so that the placement of the resonator is more flexible.

V. RESULTS AND DISCUSSION

Fig. 9 presents the optimized integration of the filtering antenna based on conventional extraction and the proposed method as shown in Fig. 9(a) and Fig. 9(b), respectively. The proposed design (SIFA) results in a much wider filtering antenna patch (16.5 mm) than the conventional extraction (2.2 mm). In addition, the latter results in a wider gap between the radiator and resonator than the former. For both designs, the optimization result in similar gaps for L_c and a difference of 0.6 mm for d (5.1 mm with the SIFA and 5.7 mm with conventional extraction). The two designs result in different surface currents; the conventional method has a vertical surface current in the narrow radiator area as shown in Fig. 10(a), and SIFA has a slant surface current in the wide radiator area as depicted in Fig. 10(b). This difference in surface current is triggered by the horizontal surface current from the stripline resonator, this excites the radiator surface current in the x direction, which is strong enough to pull the surface current

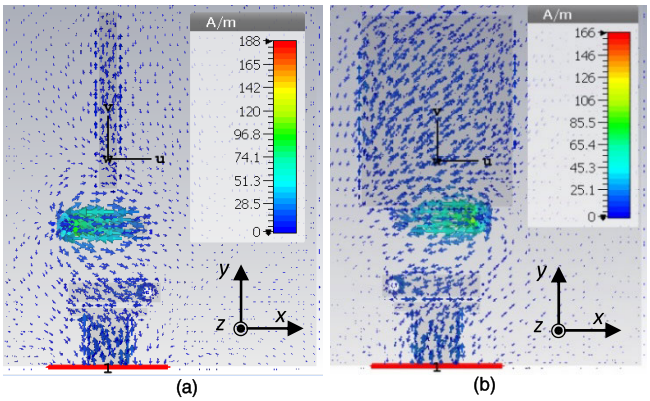

FIGURE 10. Surface current of the filtering antenna based on the (a) conventional extraction and (b) proposed method.

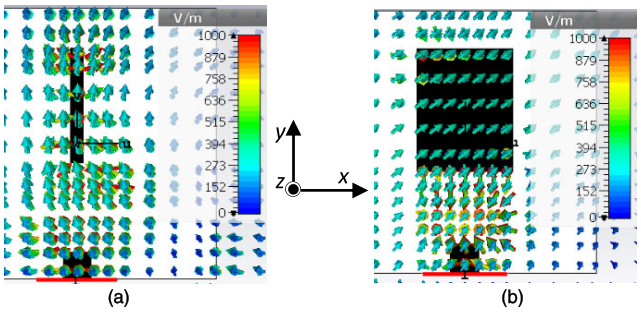

FIGURE 11. Electrical field of the filtering antenna based on the (a) conventional extraction with vertical polarization and (b) proposed method with slant polarization.

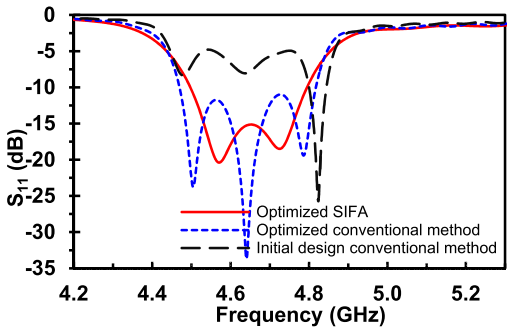

FIGURE 12. S-parameter comparison of SIFA and conventional filtering antenna with vertical polarization.

along the length of the radiator in the y direction to form a $+45°$ slant surface current in the radiator. This slant polarization result is represented by the electrical field direction as shown in Fig. 11(b). In contrast, Fig. 11(a) shows the electrical field with vertical polarization at the radiator, which resulted from the weak surface current in the x direction with the conventional method.

The conventional method and SIFA also yield different results for the S_{11} parameter, as shown in Fig. 12. The conventional method results in a filtering antenna with a third-order filtering response has three returns to zero (RZs) and two peaks, whereas, the SIFA has two RZs and one peak identical to the second-order filter response. Both designs has

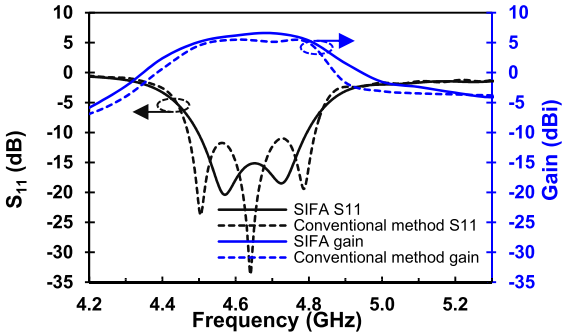

FIGURE 13. S-parameter and gain comparison of SIFA with slant polarization and conventional filtering antenna with vertical polarization.

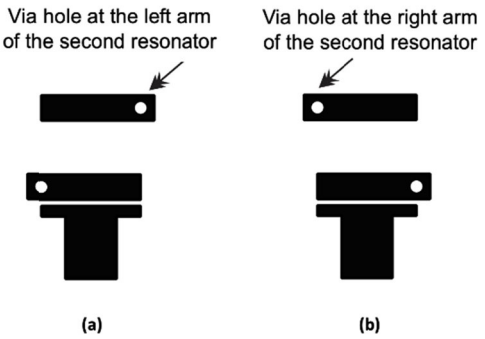

FIGURE 14. Scheme of two designs: (a) SIFA I and (b) SIFA II feedline.

a center frequency of 4.65 GHz and slightly different FBWs. The conventional filtering antenna and SIFA has -10 dB bandwidth impedances of 4.46–4.81 GHz and 4.5–4.8 GHz, respectively. The two methods also obtain different results for the gain parameter, as shown in Fig. 13. The SIFA obtains a higher but less sharp gain than the conventional method. This matched the conditions of the third-order filter, which has a better selectivity response than the second-order filter. These results demonstrate that the proposed method can successfully switch the polarization using a horizontal feed, as represented by the strip-line resonator.

A. SLANT POLARIZATION SWITCHING

The previous section demonstrates that the proposed method creates $+45°$ slant polarization instead of the vertical polarization of the conventional method. The first design of SIFA results in $+45°$ slant polarization with the via hole positioned in the right arm of the first resonator and left arm of the second resonator. This indicates that mirroring the design should result in an identical filtering antenna with orthogonal polarization. In this study, two designs are presented using CST Studio Suite, where the two antennas have a different transmission line.

In the first design's feedline (SIFA I), a via hole is located at the left arm of the second strip resonator when the via hole on the first strip resonator is set at the reversed position, as seen in Fig. 14 (a). Alternatively, for the second design feedline (SIFA II), the via position is inverted compared with SIFA I, as shown in Fig. 14 (b); thus, the mirror inversion

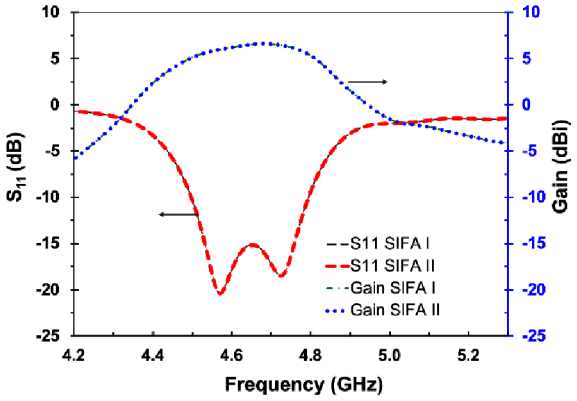

FIGURE 15. Simulation results of the reflection coefficient and gain response of SIFA I and SIFA II.

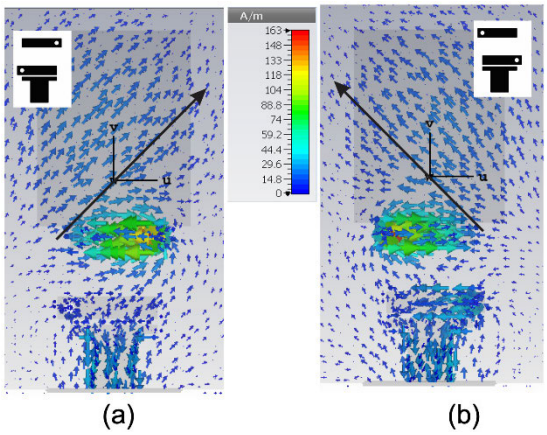

FIGURE 16. Current surface of the filtering antenna: (a) SIFA I and (b) SIFA II.

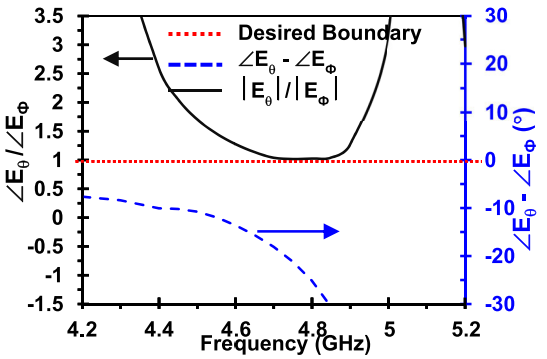

FIGURE 17. Simulation result of the phase difference dashes (blue) and magnitude ratio (solid black) of SIFA I from far-field parameter in CST.

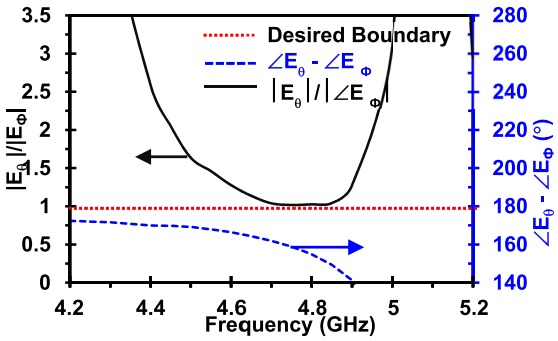

FIGURE 18. Simulation result of the phase difference (dashes blue) and magnitude ratio (solid black) of SIFA II from far-field parameter in CST.

of open and short circuit resonator feedlines is performed in the two designs. The magnitude of the reflection coefficient, S_{11}, and the gain response of the simulation results are shown in Fig. 15, from which it is obvious that the reflection coefficient (S_{11}) and the gain response of SIFA I and SIFA II are essentially identical. Moreover, both designs have a bandwidth of 4.5–4.8 GHz. with a reflection coefficient of −10 dB. In addition, the gain shows a flat response along the bandwidth and decreases sharply out of its bandwidth; for both models, the maximum value is 6.58 dBi at 4.7 GHz. However, the surface currents of both antennas at the center frequency (4.65 GHz) are in orthogonal directions, as shown in Fig. 16. In particular, SIFA I has a surface current in the 45° direction whereas, SIFA II has a surface current in the −45° direction as shown in Fig. 16(a) and Fig. 16(b) respectively. The polarization direction originates from the current movement from the via hole on the first resonator to that on the second resonator. This slanted surface current is generated from the inverted parallel open and short circuits of the resonators, and it reveals that the position of the via hole affects the surface current inclination on the rectangular radiator. The simulation results indicate that most of the surface current flows from the open circuit to short circuit and reverses direction at the first and second resonators, which forms a horizontal surface current. Moreover, some of the current flows from the via hole of the first resonator to that of the second resonator and reverses direction. Accordingly, it can be concluded that the positions of the via holes for the two resonators affect the polarization direction of the filtering antenna.

Other parameters to verify that the designs have +45° and −45° polarization can be obtained from the simulation results at the far-field using CST whereas the requirements in (1) and (2) are accomplished. The SIFA I phase difference between θ and Φ ($\angle E_\theta$ and $\angle E_\Phi$) is varied along with the bandwidth of 4.5–4.8 GHz with a value of −10° to −25° or approximately 0° (desired value). The magnitude ratio ($|E_\theta|/|E_\Phi|$) value is between 1.7 and 1.02 or near 1 (desired value); these values confirm that SIFA I has 45° polarization, as shown in Fig. 17. Meanwhile, Fig. 18 shows that SIFA II has −45° polarization from the phase difference value which is varied between 169° to 154° or near 180° (desired value), and the magnitude ratio ranges from 1.6 to 1.02 or close to 1 (desired value).

B. CONTROLLABLE BANDWIDTH AND GAIN SHAPING

The proposed design also includes an antenna with a controllable bandwidth, as shown in Fig. 19. The distance between the two resonators, d, affects the bandwidth of the antenna because the closer it is, the higher is the coupling effect that occurs, resulting in a higher value of S_{11} and wider

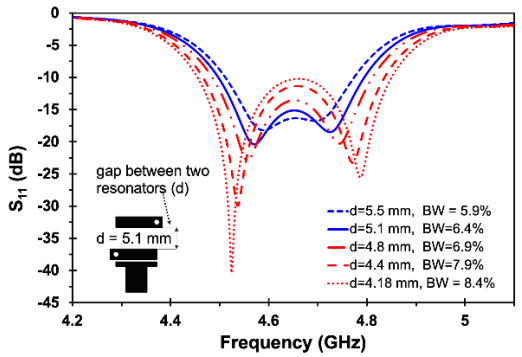

FIGURE 19. Reflection coefficient (S11) and bandwidth of SIFA I and SIFA II under the variation of the gap, d, between the resonators.

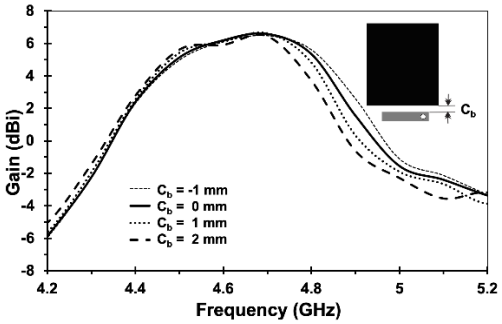

FIGURE 20. Gain shape of SIFA I and SIFA II under the variation of the gap, CB, between the radiator and the second resonator.

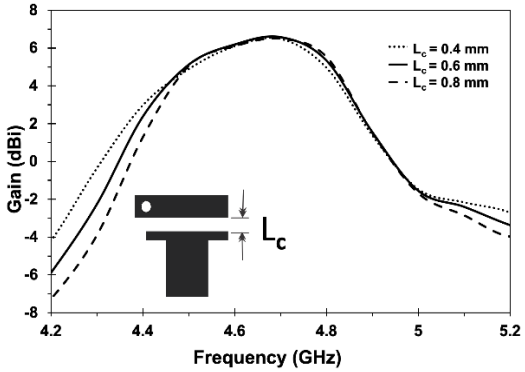

FIGURE 21. Gain shape of SIFA I and SIFA II under varied gap between the feed coupled and the first resonator, LC.

in the bandwidth. However, this d variation does not affect SIFA's center frequency and polarization. SIFA has a bandwidth range of 5.9%–8.4% with S_{11} of −10 dB and a center frequency of 4.65 GHz, and the distance between the two resonators ranges from 4.18 to 5.5 mm. The independent gain shaping of this design is evident from the parametric study. The distance effect between the second resonator and the radiator, $C_{B,}$ is depicted in Fig. 20, which shows that the gap increase will sharpen the gain at the upper frequency, but the gain at the center and lower frequency is not affected. Meanwhile, Fig. 21 shows the impact of the gap between the feed coupled and the first resonator, L_C, where the increase in L_C will sharpen the gain at the lower frequency without

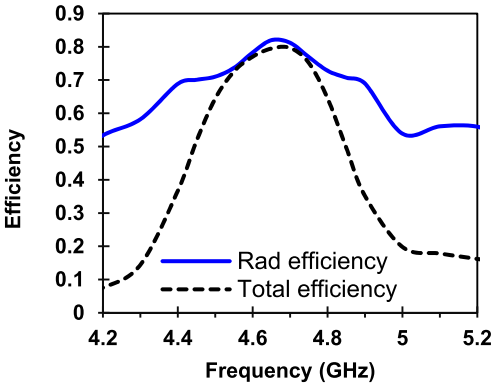

FIGURE 22. Efficiency of SIFA I and SIFA II.

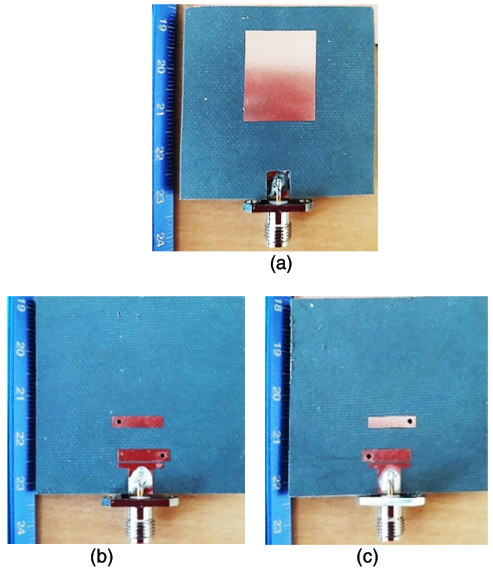

FIGURE 23. Fabrication of (a) radiator on the first layer (b) SIFA I on the second layer, and (c) SIFA II on the second layer.

affecting the gain at the center and upper frequency. It is also observed that this independent gain shaping applies to both SIFA I and SIFA II without affecting the polarization. In the simulation, the radiation efficiency of the SIFA was around 0.7–0.8 in the passband, and total efficiency was near 0.8 as shown in Fig. 22. This imperfect value can be attributed to the losses caused by the filtering structure.

C. MEASUREMENT

The simulation results of both designs are validated by fabrication and measurement. The fabrication results for SIFA I and SIFA II are shown in Fig. 23. The measurement results in Fig. 24 reveal that the −10 dB impedance bandwidth, S_{11}, of SIFA I is 4.520–4.811 GHz or shifts 20 MHz to the higher frequency compared with the simulation results. Moreover, SIFA II has a bandwidth of 4.519–4.816 GHz shifted 19 MHz to the higher frequency. For both, this constitutes a bandwidth shift of 0.4% relative to the center frequency, which can be attributed to the tolerance of fabrication and the substrate's dielectric constant.

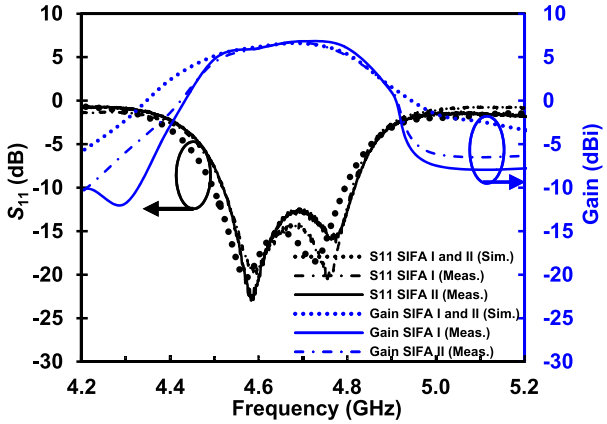

FIGURE 24. Simulation and measurement results of SIFA I and SIFA II with S11 (black curve) and gain (blue curve).

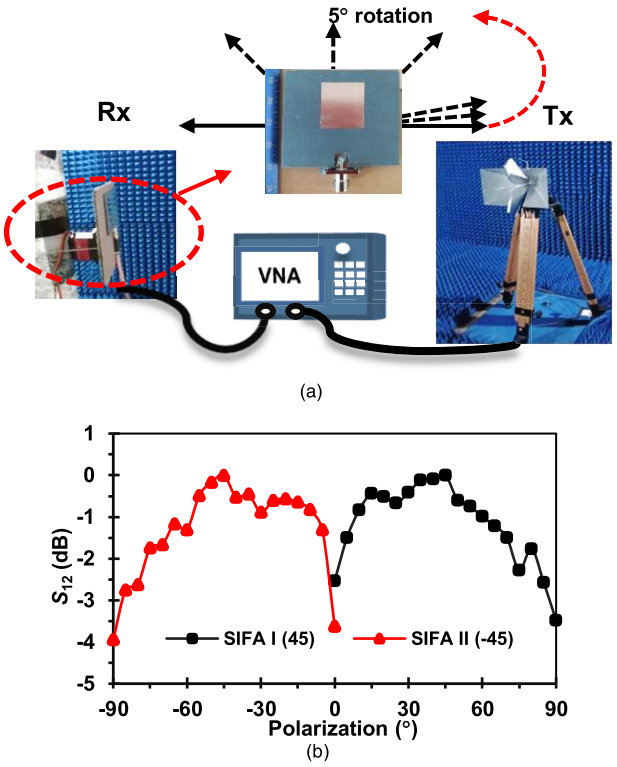

FIGURE 25. 25. (a) Measurement setup to verify the polarization of SIFA I and SIFA II and (b) normalized receiving performance (S_{12}) measured for SIFA I (black line) and SIFA II (red line) with different polarizations at 4.65 GHz.

To verify that SIFA I and SIFA II have a 45° and −45° polarization, the power received performance, S_{12}, is measured in an anechoic chamber with a horn antenna operating as a transmitter and the filtering antennas functioning as the receiver. The antennas are separated using a gap of 2 m; the measurement setup is shown in Fig. 25 (a). The receiving antennas are set for a range of polarizations, specifically, 0° – 90° for SIFA I in an anticlockwise direction and 0 to −90° for SIFA II in a clockwise direction in increments of 5°. Fig. 25 (b) shows that the power received increases from 0° to 45° and decreases from 45° to 90° in SIFA I,

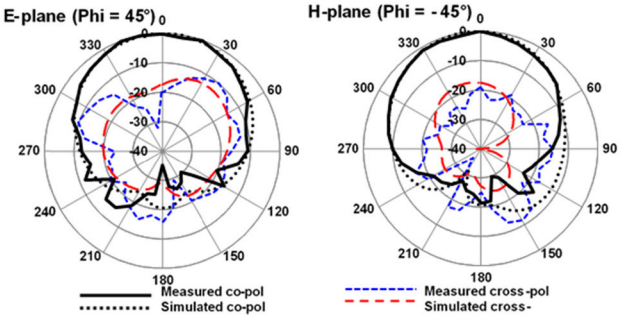

FIGURE 26. Simulation and measurement results of SIFA I radiation pattern at 4.65 GHz.

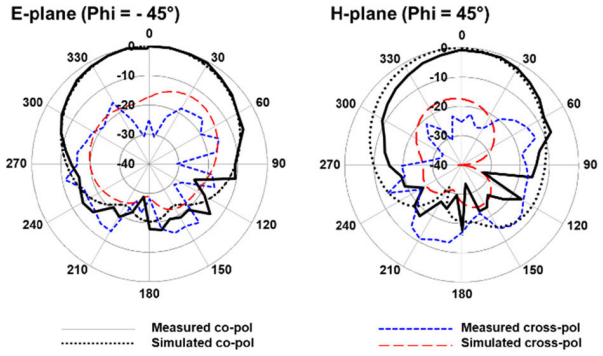

FIGURE 27. Simulation and measurement results of SIFA II radiation pattern at 4.65 GHz.

whereas in SIFA II, the S_{12} value increases from 0 to −45° but subsequently decreases from −45° to −90°. The S_{12} measurement proves that SIFA I and SIFA II have 45° and −45° polarization, respectively. Gain measurements are then conducted with the horn antenna polarization set to 45° for SIFA I and −45° for SIFA II. Fig. 24 shows the simulation and measurement results for the gain parameter, from which it is apparent that for SIFA I and SIFA II, the maximum gain is 6.82 and 6.69 dBi at 4.7 GHz, respectively. These values are 0.1 and 0.2 dB higher than the simulation results. Furthermore, the measurement results show a flat gain along 4.5–4.8 GHz, which decreases sharply out of the bandwidth.

The radiation patterns of SIFA I and SIFA II at 4.65 GHz are shown in Fig. 26 and Fig. 27, respectively; it is evident that the simulation results for both antennas have an identical radiation pattern. The measurement results of co-polarization (Phi = +45° and −45° slant polarization for SIFA I and SIFA II, respectively) and the measurement results for cross polarization (Phi = −45° and +45° slant polarization for SIFA I and SIFA II, respectively) are in accordance with the simulation results, which shows a unidirectional radiation pattern in the E-plane and H-plane at 4.65 GHz. The measurement results in the E-plane and H-plane revealed a cross polarization of less than −20 dB at the 2° and 10° main lobe, respectively. The horizontal and vertical HPBWs of SIFA I and SIFA II are around 80° and 74°, respectively.

Table 1 compares the result of the present study and previous works. The present study proposes a new method for slant polarization that uses two strip resonators with via

TABLE 1. Comparison of the proposed antenna with other dual polarized antennas.

Ref.	Polarization method	Gain (dBi)	Filtering Response	Controllable Bandwidth
[8]	V/H* crossed radiator	9	Yes	No
[9]	SP** crossed dipole	8-9	Yes	No
[10]	SP crossed dipole	7.8/8.6	No	No
[11]	SP radiator rotation	7/7.2	Yes	No
[12]	SP crossed slot	7	Yes	No
[22]	SP using characteristic mode	2	No	No
This work	SP using resonator	6.8/6.9	Yes	5.9%-8.4%

*V/H = Vertical/Horizontal, **SP = Slant Polarization

holes. It also provides a filtering response and controllable bandwidth. Although the proposed result does not have a high gain compare with the first five works, it is because those works use a reflector, three layers and an air gap which results in unwieldy designs.

VI. CONCLUSION

In this paper, two SIFAs were proposed and their performances were verified using simulations and measurements. The design implemented two resonators in the transmission lines, producing two inverted parallel resonators that fed the rectangular radiator, which was also parallel to the two resonators. The filter synthesis is based on a third-order filter with a fractional bandwidth of 6.45% and ripple of 0.2 dB. Both antennas operate at 4.65 GHz, have a fractional bandwidth of 6.45%, and a reflection coefficient of −10 dB; moreover, they achieve 45° (SIFA I) and −45° (SIFA II) slant polarization and a controllable bandwidth from 5.9% to 8.4%. The orthogonal polarization direction is switched by the location of the via hole. The antennas show a flat gain within the operational bandwidth with a maximum gain of 6.82 (SIFA I) and 6.69 dBi (SIFA II) at 4.7 GHz and the upper and lower frequency's gain sharpness can be individually controlled without affecting the gain at the center frequency. The symmetric inverted structure of both antennas generates an identical S_{11}, gain, and radiation patterns but with orthogonal polarization. These antennas can be applied for 5G at the middle band.

REFERENCES

[1] J. J. A. Lempiainen and J. K. Laiho-Steffens, "The performance of polarization diversity schemes at a base station in small/micro cells at 1800 MHz," *IEEE Trans. Veh. Technol.*, vol. 47, no. 3, pp. 1087–1092, Aug. 1998.
[2] K. Nishimori, Y. Makise, M. Ida, R. Kudo, and K. Tsunekawa, "Channel capacity measurement of 8×2 MIMO transmission by antenna configurations in an actual cellular environment," *IEEE Trans. Antennas Propag.*, vol. 54, no. 11, pp. 3285–3291, Nov. 2006.
[3] F. Challita, P. Laly, M. Yusuf, E. Tanghe, W. Joseph, M. Lienard, D. P. Gaillot, and P. Degauque, "Massive MIMO communication strategy using polarization diversity for industrial scenarios," *IEEE Antennas Wireless Propag. Lett.*, vol. 19, no. 2, pp. 297–301, Feb. 2020.
[4] L. Vallozzi, "Patch antenna with slanted ±45° dual polarization and performance comparison with H/V diversity," in *Proc. 10th Eur. Conf. Antennas Propag. (EuCAP)*, Apr. 2016, pp. 1–5.
[5] Z. Niu and Y. Fan, "Dual-polarized low-profile filtering patch antenna without extra circuit," *IEEE Access*, vol. 7, pp. 106011–106018, 2019.
[6] W. Duan, X. Y. Zhang, Y.-M. Pan, J.-X. Xu, and Q. Xue, "Dual-polarized filtering antenna with high selectivity and low cross polarization," *IEEE Trans. Antennas Propag.*, vol. 64, no. 10, pp. 4188–4196, Oct. 2016.
[7] W. Yang, M. Xun, W. Che, W. Feng, Y. Zhang, and Q. Xue, "Novel compact high-gain differential-fed dual-polarized filtering patch antenna," *IEEE Trans. Antennas Propag.*, vol. 67, no. 12, pp. 7261–7271, Dec. 2019.
[8] C. Hua, R. Li, Y. Wang, and Y. Lu, "Dual-polarized filtering antenna with printed jerusalem-cross radiator," *IEEE Access*, vol. 6, pp. 9000–9005, 2018.
[9] W. Duan, Y. F. Cao, Y.-M. Pan, Z. X. Chen, and X. Y. Zhang, "Compact dual-band dual-polarized base-station antenna array with a small frequency ratio using filtering elements," *IEEE Access*, vol. 7, pp. 127800–127808, 2019.
[10] Y. Liu, S. Wang, N. Li, J.-B. Wang, and J. Zhao, "A compact dual-band dual-polarized antenna with filtering structures for sub-6 GHz base station applications," *IEEE Antennas Wireless Propag. Lett.*, vol. 17, no. 10, pp. 1764–1768, Oct. 2018.
[11] J.-F. Li, D.-L. Wu, G. Zhang, Y.-J. Wu, and C.-X. Mao, "Compact dual-polarized antenna for dual-band full-duplex base station applications," *IEEE Access*, vol. 7, pp. 72761–72769, 2019.
[12] K. Xue, D. Yang, C. Guo, H. Zhai, H. Li, and Y. Zeng, "A dual-polarized filtering base-station antenna with compact size for 5G applications," *IEEE Antennas Wireless Propag. Lett.*, vol. 19, no. 8, pp. 1316–1320, Aug. 2020.
[13] S. Martin-Anton and D. Segovia-Vargas, "Fully planar dual-polarized broadband antenna for 3G, 4G and sub 6-GHz 5G base stations," *IEEE Access*, vol. 8, pp. 91940–91947, 2020.
[14] A. Dastranj and B. Abbasi-Arand, "High-performance 45° slant-polarized omnidirectional antenna for 2–66-GHz UWB applications," *IEEE Trans. Antennas Propag.*, vol. 64, no. 2, pp. 815–820, Feb. 2016.
[15] H. Huang, S. Gao, S. Lin, and L. Ge, "A wideband water patch antenna with polarization diversity," *IEEE Antennas Wireless Propag. Lett.*, vol. 9, no. 7, pp. 1113–1117, 2020.
[16] Q.-X. Chu, Y.-L. Chang, and J.-P. Li, "Communication crisscross-shaped ±45° dual-polarized antenna with enhanced bandwidth for base stations," *IEEE Trans. Antennas Propag.*, early access, Aug. 21, 2020, doi: 10.1109/TAP.2020.3017098.
[17] Y. M. Pan, S. Y. Zheng, and B. J. Hu, "Singly-fed wideband 45° slant-polarized omnidirectional antennas," *IEEE Antennas Wireless Propag. Lett.*, vol. 13, pp. 1445–1448, 2014.
[18] X. Quan, R. Li, Y. Fan, and D. E. Anagnostou, "Analysis and design of a 45° slant-polarized omnidirectional antenna," *IEEE Trans. Antennas Propag.*, vol. 62, no. 1, pp. 86–93, Jan. 2014.
[19] Y. Fan, R. Li, and Y. Cui, "Development of polarisation reconfigurable omnidirectional antennas using crossed dipoles," *IET Microw., Antennas Propag.*, vol. 13, no. 4, pp. 485–491, Mar. 2019.
[20] M. Li, X. Chen, A. Zhang, W. Fan, and A. A. Kishk, "Split-ring resonator-loaded baffles for decoupling of dual-polarized base station array," *IEEE Antennas Wireless Propag. Lett.*, vol. 19, no. 10, pp. 1828–1832, Oct. 2020.
[21] Y. P. Selvam, L. Elumalai, M. G. N. Alsath, M. Kanagasabai, S. Subbaraj, and S. Kingsly, "Novel frequency- and pattern-reconfigurable rhombic patch antenna with switchable polarization," *IEEE Antennas Wireless Propag. Lett.*, vol. 16, pp. 1639–1642, 2017.
[22] Y. Yan, A. Sharif, J. Ouyang, C. Zhang, and X. Ma, "UHF RFID handset antenna design with slant polarization for IoT and future 5G enabled smart cities applications using CM analysis," *IEEE Access*, vol. 8, pp. 22792–22801, 2020.
[23] D. A. Cahyasiwi, F. Y. Zulkifli, and E. T. Rahardjo, "Stacked interdigital filtering antenna with slant polarization," in *Proc. IEEE Conf. Antenna Meas. Appl. (CAMA)*, Oct. 2019, pp. 275–278.
[24] W. Stutzman and G. Thiele, *Antenna Theory and Design*, 3rd ed. Hoboken, NJ, USA: Wiley, 2013.
[25] G. L. Matthaei, "Interdigital, band-pass filter," in *PGMTT Nat. Symp. Dig.*, 1961, pp. 41–45.
[26] G. L. Matthaei, L. E. O. Young, and E. M. T. Jones, *Microwave Filters, and Coupling Structures*. Princeton, NJ, USA: Artech House, 1985.
[27] J. S. Hong and M. J. Lancaster, *Microstrip Filters for RF/Microwave Applications*. New York, NY, USA: Wiley, 2001.

DWI ASTUTI CAHYASIWI (Student Member, IEEE) was born in Jakarta, Indonesia, in 1974. She received the bachelor's and M.T. degrees in telecommunication engineering from Universitas Indonesia, in 1997 and 2009, respectively, where she is currently pursuing the Ph.D. degree. Her research interests include integration design of antenna and filter, metasurface, and microwave circuits. She was a recipient of the Best Student Paper Award from the 2019 IEEE Conference on Antenna Measurement and Applications.

FITRI YULI ZULKIFLI (Senior Member, IEEE) was born in Banda Aceh, Indonesia, in 19 July 1974. She received the bachelor's degree in electrical engineering from Universitas Indonesia, in 1997, the M.Sc. degree from the Department of Telecommunication and Information Technology, University of Karlsruhe, Germany, in 2002, and the Ph.D. degree *(cum laude)* in electrical engineering from Universitas Indonesia, in 2009. She received the Deutscher Akademischer Austauschdienst (DAAD) scholarship to study her master's degree in Germany.

In 1997, she joined the Antenna Propagation and Microwave Research Group (AMRG) UI and became a Lecturer, in 1998. She has published more than 190 articles in international/national journals and conference proceedings. She has been involved in more than 40 granted researches. Her research interests include antenna, propagation, microwave, and in the field of electromagnetic.

Prof. Zulkifli is involved in many teamwork activities and also involved in organizing committee in many seminars and workshops. She has been a Secretary and a Treasurer of the IEEE Joint Chapter MTT/AP. In 2010, she was a Treasurer of the IEEE Joint Chapter MTT/AP, and then from 2011 to 2012, she has become the Joint Chapter Chair. From 2013 to 2016, she was the Coordinator for technical activity in IEEE Indonesia Section. From 2017 to 2018, she was the IEEE Indonesia Section Chair. From 2019 to 2020, she serves as a Committee Member for the R10 Conference and Technical Seminar and Conference Quality Management. She is currently an Executive Committee of the joint chapter MTT/AP-S and also the Head of the Advisory Board of the IEEE Indonesia Section. She was a recipient of the Best Lecturer Award (Dosen Berprestasi) from Universitas Indonesia, in 2011, and achieved Fourth Place for the Best Lecturer Award from the Government of Republic Indonesia, in 2011.

EKO TJIPTO RAHARDJO (Member, IEEE) was born in Pati, Indonesia, in 22 April 1958. He received the Ir. (Insinyur) degree from Universitas Indonesia, Depok, Indonesia, in 1981, the M.S. degree from the University of Hawai'i at Manoa, Honolulu, HI, USA, in 1987, and the Ph.D. degree from Saitama University, Urawa, Japan, in 1996, all in electrical engineering.

Since 1982, he has been a Teaching Assistant with the Department of Electrical Engineering, Universitas Indonesia. Since 2005, he has also been appointed as a Professor in electrical engineering. He was the Chairman of The University Senate, Universitas Indonesia, from 2011 to 2012, the Head of the Department of Electrical Engineering, Universitas Indonesia, from 2004 to 2008, and the Executive Director of the Quality Undergraduate Education (QUE), Department of Electrical Engineering, Universitas Indonesia, from 1999 to 2004, where he was also the Head of the Telecommunication Laboratory, from 1997 to 2004. Since 2003, he has been the Director of Antenna Propagation and Microwave Research Group (AMRG), Universitas Indonesia. He has been published and presented more than 100 research articles both national and international journals and symposiums. His research interests include antenna engineering, wave propagation, microwave circuits and communication systems, and telecommunication system regulations.

Prof. Rahardjo is a member of the IEEE Antenna and Propagation Society (AP-S) and the IEEE Microwave Theory and Technique Society (MTTS). He has been a member of the International Steering Committee (ISC) of Asia–Pacific Microwave Conference (APMC), since 2010, and the International Advisory Board of International Symposium on Antenna and Propagation (ISAP), since 2012. He was a recipient of the Indonesian Government Scholarship through MUCIA, from 1984 to 1987, the Hitachi Scholarship, from 1992 to 1996, the Young Researcher's Award from Universitas Indonesia, in 1996, the Second Winner of Best Researcher Award in Science and Technology from Universitas Indonesia, in 2009, and the Second Winner of Best Teaching Award from Universitas Indonesia, in 2010. He was the Founder of the IEEE Joint Chapter MTT-S/AP-S Indonesia. He has served as the President for the IEEE Joint Chapter MTT-S/AP-S, from 2009 to 2010, and the IEEE Indonesia Section, from 2014 to 2015. He is the General Chairman of the Indonesia Malaysia Microwave and Antenna Conference (IMMAC), Depok, in 2010, and the Indonesia Japan Joint Scientific Symposium (IJJSS), Bali, in 2010, and the General Co-Chairman of the Indonesia Japan Joint Scientific Symposium (IJJSS), Chiba, Japan, in 2012. In addition, he also been the General Chair of the 1st Indonesia—Japan workshop on Antennas and Wireless Technology (IJAWT), Depok, in 2017, and the 2019 IEEE International Conference on Antenna Measurements and Applications (CAMA), Bali, in October 2019.